Investigation of the influence of the reabsorption of radiation in spectral lines on the gain coefficient on transitions of Li-like ions in a recombining laser plasma

A. L. Godunov, V. A. Makhrov, A. Yu. Sechin, A. N. Starostin, and A. E. Stepanov

Troitsk Institute of Innovative and Thermonuclear Research, 142092 Troitsk, Moscow Region, Russia
(Submitted 1 November 1995)
Zh. Éksp. Teor. Fiz. **109**, 2064–2077 (June 1996)

A detailed self-consistent model of the population kinetics of the levels of aluminum ions is developed with consideration of the gas dynamics of the plasma and radiation transfer. It is used to analyze the experimental results and to investigate the accuracy of describing the reabsorption of radiation in spectral lines within the Sobolev approximation. It is shown that for locally optically thick lines the photon-escape-probability approximation is in satisfactory agreement with the results of a numerical solution of a combined system of equations describing the kinetics and resonant radiation transfer in an inhomogeneous moving plasma. © *1996 American Institute of Physics.* [S1063-7761(96)01106-7]

1. INTRODUCTION

The progress which has been achieved in recent years in inducing lasing in the vacuum-ultraviolet and soft x-ray regions is based on the use of two principal pumping schemes. They are the collisional scheme,[1] in which the upper working level is populated by electron impact, and the recombination scheme, in which population inversion is achieved owing to the preferential populating of the upper levels as a result of ternary recombination. The recombination scheme for creating a population inversion in hydrogenic ions has attracted great attention both because of the possibility, in principle, of obtaining laser action in the range of wavelengths corresponding to the "water window" and because of the relative simplicity of the scheme of levels and, therefore, of the entire atomic model.

The investigations in Refs. 2–4 showed that a very important factor lowering the gain coefficient is the reabsorption of radiation in spectral lines, which is especially strong on resonant 2–1 transitions. A detailed description of this process requires a combined solution of the gas-dynamic equations, the atomic model, and the radiation-transfer equation. Such a model is very complicated and costly even in the case of one-dimensional geometry. An alternative approach is to use the machinery of photon escape probabilities. In the case of a plasma with large velocity gradients, there is a possibility for significantly simplifying the calculation of escape probabilities, which was first noted by Sobolev[5] and was subsequently generalized in Refs. 6–8 and then further generalized to the case of three-dimensional flow.[9]

Along with the recombination schemes based on hydrogen-like ions, schemes with Li-like ions are also widely investigated. As evaluations have shown, Li-like ions potentially impose weaker constraints on the parameters of the pump laser for progressing to lasing in the short-wavelength region than do hydrogenic ions. The influence of various physical approximations in the theoretical model on the gain coefficient in Li-like aluminum was analyzed in Ref. 10 under the experimental conditions in Ref. 11. Just as in the case of hydrogen-like ions, the reabsorption of radiation in spectral lines strongly influenced the gain coefficient. The calculations in Ref. 10 were performed in the photon-escape-probability approximation.[9] However, the question of the accuracy of this approach as applied to recombination schemes for creating a population inversion in Li-like ions remains open.

A detailed model of the population kinetics of the levels of aluminum ions is developed in this paper with consideration of the gas dynamics of the plasma and radiation transfer. It is then used to analyze the results of the experiments in Ref. 11 and to investigate the accuracy of describing the reabsorption of radiation in spectral lines within the Sobolev approximation.

2. PHYSICAL MODEL

The numerical model which we used to interpret the experimental data from Ref. 11 regarding the attainment of amplification in Li-like aluminum calls for solving the level-by-level kinetic equations for all stages of the ionization of aluminum, beginning from the N-like ions, together with the equations of one-dimensional gas-dynamics and radiation transfer in the spectral lines and the continuum in cylindrical geometry.

The gas dynamics of a plasma are described in the single-fluid two-temperature approximation. The calculations were performed within one-dimensional cylindrical geometry, which is an adequate approximation in the case of the geometry of the irradiation of the fiber target described in Ref. 11. This is confirmed both by the two-dimensional calculations in Ref. 2 and by our results. The continuity, motion, and energy equations for electrons and ions are written in the following manner ($\nu=0$, 1, 2 for the cases of planar, cylindrical, and spherical geometry, respectively):

$$\frac{d\rho}{dt}=-\rho\frac{1}{r^{\nu}}\frac{\partial}{\partial r}(r^{\nu}v), \tag{1}$$

$$\rho\frac{dv}{dt}=-\frac{\partial\,(p_e+p_i+\omega)}{\partial r}, \tag{2}$$

 1063-7761/96/061112-08$10.00

$$\frac{d\epsilon_e}{dt}=-\frac{p_e}{\rho}\frac{1}{r^\nu}\frac{\partial}{\partial r}(r^\nu v)+H_e-Q_{ei}+Q_{\text{las}}+Q_{\text{rad}}+Q_{\text{int}}, \tag{3}$$

$$\frac{d\epsilon_i}{dt}=-\frac{p_i+\omega}{\rho}\frac{1}{r^\nu}\frac{\partial}{\partial r}(r^\nu v)+H_i+Q_{ei}. \tag{4}$$

Here

$$\frac{d}{dt}=\frac{\partial}{\partial t}+v\frac{\partial}{\partial r},$$

ρ is the density, p_e and p_i are the electron and ion pressures, ω is the pressure associated with the introduction of an artificial viscosity, v is the velocity, and ϵ_e and ϵ_i are the specific internal energies of the electrons and ions. In Eqs. (3) and (4) the terms H_e and H_i describe the electronic and ionic thermal conductivities, Q_{las} is the absorption of laser radiation in the plasma, Q_{rad} is the bulk loss of energy to radiation, and Q_{int} is the energy expended on ionization and excitation. The system of equations (1)–(4) was solved using a Lagrangian difference scheme.

The value of the electronic thermal conductivity was calculated using the formula

$$\kappa_e=\frac{\kappa_e^{cl}}{1+\kappa_e^{cl}\phi},\quad \phi=\frac{|\nabla T_e|}{2\times 10^{37} f T_e^{3/2}\rho\langle Z\rangle/\langle A\rangle}, \tag{5}$$

where all the parameters are in cgs units, $f=\text{const}$ is a dimensionless parameter introduced to limit the thermal conductivity flux (in all the results presented we set $f=0.1$ or 0.2), $\langle Z\rangle$ is the mean charge, $\langle A\rangle$ is the mean atomic weight of the ions, and the value of κ_e^{cl} was taken from Ref. 12.

The classical expression[12] was also taken for Q_{ei}, which takes into account the relaxation of the electron and ion temperatures.

The system of gas-dynamic equations is closed by the equation of state of an ideal gas.

When populations are calculated with consideration of the radiation transfer in the lines and the continuum, the influence of the radiation field on the population kinetics is determined by the $\bar{J}_{ul}$:

$$\bar{J}=\frac{1}{4\pi}\int d\Omega\int d\omega I(r,\omega,\Omega)\Phi_{ul}\left(\omega-\omega_0\frac{\Omega\mathbf{v}(\mathbf{r})}{c}\right), \tag{6}$$

where $I(r,\omega,\Omega)$ is the radiated intensity, which depends on the spatial point, the frequency, and the solid angle, Φ_{ul} is the profile of the spectral line of the $u\to l$ transition, and Ω is a unit vector in the photon propagation direction. In the present work we used the approximation of complete frequency redistribution;[13] therefore, $\Phi_{lu}=\Phi_{ul}$ and $J_{lu}=J_{ul}$. The photoionization rate equals

$$R_{lu}=\int d\Omega\int_{I_l}^{\infty}\frac{d\omega}{\omega}\sigma_{lu}^{\text{ph}}(\omega)I(r,\omega,\Omega), \tag{7}$$

where I_l is the ionization potential of level l, and $\sigma_{lu}^{\text{ph}}(\omega)$ is the photoionization cross section. The radiated intensity found from the equation

$$\sqrt{1-\gamma^2}\left(\mu\frac{\partial I}{\partial r}+\frac{1-\mu^2}{r}\frac{\partial I}{\partial\mu}\right)=-kI+\varepsilon, \tag{8}$$

where μ and γ are the cosines of the angles specifying the photon flight direction in cylindrical geometry (see, for example Ref. 14), k is the total absorption coefficient, which is the sum of the absorption in the spectral line (or several lines, if their profiles overlap) and the continuum, and ϵ is the total emissivity in the spectral lines and the continuum. Emission and absorption in the continuum are associated with bremsstrahlung and absorption, as well as with recombination emission and the absorption of photons upon photoionization. The nonlinear system of equations (1)–(6) was solved using Newton's method, which ensured sufficiently rapid convergence of the iteration process over a broad range of plasma parameters.

The populations of the various states of the Al ions are found from the system of kinetic equations

$$\frac{d\mathbf{C}(r,t)}{dt}=\mathbf{K}\mathbf{C}(r,t). \tag{9}$$

The vector $\mathbf{C}(r,t)$ describes the set of relative populations of all the states taken into account at the time t at a certain point in space r: $\mathbf{C}(r,t)=\{C_1(r,t),\ldots,C_L(r,t)\}$, and $C_l(r,t)=n_l(r,t)/n_{\text{tot}}(r,t)$, where n_l is the population of level l, and n_{tot} is the total density of all the ions, i.e., $n_{\text{tot}}=\Sigma_l n_l$. The matrix $\mathbf{K}$ describes all the possible elementary processes which lead to transitions between different states ($l<u$):

$$K_{lu}(r,t)=n_e\langle\sigma v\rangle_{ul}^{q}+A_{ul}+\alpha_{ul}^{\text{rec}}+B_{ul}\bar{J}_{ul}, \tag{10}$$

$$K_{ul}(r,t)=n_e\langle\sigma v\rangle_{lu}^{\text{ex}}+n_e\langle\sigma v\rangle_{lu}^{\text{ion}}+B_{lu}\bar{J}_{lu}+R_{lu}, \tag{11}$$

where n_e is the electron density, $\langle\sigma v\rangle^{\text{ex}}$ and $\langle\sigma v\rangle^{q}$ are the rates of excitation and quenching of the transition by electrons, α^{rec} is the total recombination rate, which is the sum of the rates of photorecombination, three-body recombination, and induced photorecombination, $\langle\sigma v\rangle^{\text{ion}}$ is the rate of ionization by electrons of the lower level l with a transition to level u, the A_{ul} are the Einstein coefficients for the probability of a spontaneous radiative transition, B_{ul} and B_{lu} are the Einstein coefficients for induced emission, and R_{lu} is the photoionization rate.

The following set of levels was used in this work. The 16 levels nlj (up to $n=4$) were taken into account for the hydrogenic ions. Twelve levels (up to $n=4$) were taken into account for the He-like lines. A total of 44 levels were taken into account for the Li-like ions: the 35 levels nlj with $n\leqslant 6$ and 9 hydrogenic levels from $n=7$ to $n=15$ without splitting with respect to lj. The energies of the levels with $n\leqslant 6$, as well as the oscillator strengths for the transitions between these levels and the levels of the He-like ions, were calculated in the Hartree–Fock approximation with consideration of relativistic corrections of order α^2 (Ref. 15) and agree fairly well with the data from Ref. 16. The formulas for hydrogenic ions were used for transitions involving levels with $n>6$. A scheme with 11 levels [$2s^2{}^1S$, $2s2p^1P$, $2s2p^3P$, $2s3s^3S$, $2s3s^1S$, $2s3p^3P$, $2s3p^1P$, $2s3d^3D$, $2s3d^1D$, $^3(n=4)$, and $^1(n=4)$; the last two levels represent combinations of all the triplet and singlet states of a level with $n=4$] was used for the Be-like ions. A scheme of five levels ($2s^22p$, $2s^23s$, $2s^23p$, $2s^23d$, and $2s^22p^2$) was em-

ployed for the B-like ions, a scheme of five levels ($2s^2 2p^2$, $2s^2 2p 3s$, $2s^2 2p 3p$, $2s^2 2p 3d$, and $2s^2 2p^3$) was also employed for the C-like ions, and a five-level scheme ($2s^2 2p^3$, $2s^2 2p^2 3s$, $2s^2 2p^2 3p$, $2s^2 2p^2 3d$, and $2s^2 2p^4$) was likewise employed for the N-like ions. The remaining aluminum ionization multiplicities were represented by the ground states. The oscillator strengths of transitions between levels from Be-like ions to neutral atoms were calculated using the Atom program,[17] and the energies of the levels of these ions were taken from the Tables in Ref. 18.

The coefficients B_{ul} for spontaneous radiative transitions are expressed in terms of the oscillator strengths for absorption f_{lu}:

$$\frac{g_u B_{ul}}{g_l f_{lu}} = A_0 \left(\frac{\Delta E_{lu}}{\mathrm{Ry}} \right)^2, \tag{12}$$

where $A_0 = \mathrm{Ry}\, \alpha^3/\hbar = 8.055 \times 10^9\ \mathrm{s}^{-1}$, Ry is the ionization potential of a hydrogen atom, g_u and g_l are statistical weights, and ΔE_{lu} is the difference between the energies of the levels (the energy of the transition). In calculating the gas dynamics, the reabsorption of radiation in the spectral lines was taken into account by photon escape probabilities[6,9] calculated in the Sobolev approximation:

$$\begin{aligned}\theta(\xi;\gamma_1,\gamma_2,\gamma_3) = & \int_{\gamma_1}^{\gamma_2} dt \frac{|t|}{\xi}\left[1-\exp\left(-\frac{\xi}{|t|}\right)\right] \\ & \times \frac{[(\gamma_2-\gamma_1)(\gamma_3-t)]^{-1/2}}{\pi} K(\chi_1) \\ & + \int_{\gamma_2}^{\gamma_3} dt \frac{|t|}{\xi}\left[1-\exp\left(-\frac{\xi}{|t|}\right)\right] \\ & \times \frac{[(\gamma_3-\gamma_2)(t-\gamma_1)]^{-1/2}}{\pi} K(\chi_2),\end{aligned}$$

$$\chi_1 = \sqrt{\frac{(t-\gamma_1)(\gamma_3-\gamma_2)}{(\gamma_2-\gamma_1)(\gamma_3-t)}}, \quad \chi_2 = \sqrt{\frac{(\gamma_2-\gamma_1)(\gamma_3-t)}{(t-\gamma_1)(\gamma_3-\gamma_2)}}. \tag{13}$$

Here γ_1, γ_2, and γ_3 are three eigenvalues of the rate of deformation tensor Q_{ij}, which are ordered so that $\gamma_1 < \gamma_2 < \gamma_3$,

$$Q_{ij} \equiv \frac{1}{2}\left(\frac{\partial v_i}{\partial r_j} + \frac{\partial v_j}{\partial r_i}\right), \quad Q = Q_{ij} n_i n_j, \tag{14}$$

ξ is the "reduced" optical thickness,[9] which is related to the optical thickness τ by the expression

$$\tau = \tau(\mathbf{r},\mathbf{n}) = \frac{\xi}{|Q|}, \quad \xi = \frac{2\pi k c}{\omega_0}, \tag{15}$$

and K is the complete elliptic integral of the first kind. In cylindrical geometry the set of three eigenvalues of the rate of deformation tensor equals $(0, \partial v/\partial \tau, v/r)$. The system of kinetic equations is then simplified:

$$K_{lu}(r,t) = n_e \langle \sigma v \rangle_{ul}^{q} + \theta A_{ul} + \alpha_{ul}^{\mathrm{rec}}, \tag{16}$$

$$K_{ul}(r,t) = n_e \langle \sigma v \rangle_{lu}^{\mathrm{ex}} + n_e \langle \sigma v \rangle_{lu}^{\mathrm{ion}}. \tag{17}$$

Under the experimental conditions considered in this paper photoionization can be disregarded, and it is omitted in the system of kinetic equations. Despite the apparent complexity of the formula for calculating the photon escape probability θ, its calculation for all the radiative transitions taken into account increases the calculation time by only 10–20%. At the same time, the approach developed in Refs. 6 and 9 is equally applicable in the case of two- and three-dimensional flows, making it possible to use the same program to simulate the two-dimensional gas dynamics of a laser plasma. Special tests showed that a calculation using Eq. (13) gives values of θ_{ul} that are identical to those obtained in Ref. 2 for the special case of one-dimensional geometry.

For transitions with $\Delta n \neq 0$ the excitation rate was calculated using the semi-empirical Van Regemorter equation,[19] which has the following form for a $l \to u$ transition:

$$\langle \sigma v \rangle_{lu} \left[\frac{\mathrm{cm}^3}{\mathrm{s}}\right] = (3.15 \times 10^{-7}) f_{lu} \left(\frac{\mathrm{Ry}}{\Delta E_{lu}}\right)^{3/2} \sqrt{\beta} \times \exp(-\beta) p(\beta), \tag{18}$$

where $\beta = \Delta E_{lu}/T_e$. When $\beta \ll 1$, we have $p(\beta) = -(\sqrt{3}/2\pi)\mathrm{Ei}(-\beta)$, where $\mathrm{Ei}(-\beta)$ is an exponential integral; for $\beta \geqslant 1$ we obtain $p(\beta) = 0.2$. In the program we used the formula

$$\begin{aligned} p(\beta) = & 0.2757 \exp(-1.3\beta)(-\ln\beta + \beta - 0.5772) \\ & + 0.2[1 - \exp(-4.5\beta)], \end{aligned} \tag{19}$$

which provides for adequate interpolation. For transitions between nearby levels with $\Delta n = 0$ ($nlj \leftarrow nl'j'$) we used an approximate formula from Ref. 20 based on the Bethe–Born approximation, which gives values differing from those calculated from the Van Regemorter equation by no more than a factor of 2:

$$\langle \sigma v \rangle_{lu} = (2.41 \times 10^{-7}) \frac{f_{lu}}{Z^2} \sqrt{\frac{\mathrm{Ry}}{\Delta T_e}} \frac{1 + E_1(\beta)}{\ln 4} \exp(-\beta), \tag{20}$$

where $f_{lu} = f_{lu}[\Delta E_{lu}/Z^2 \mathrm{Ry}]$ is the reduced oscillator strength, $E_1(x)$ is the first exponential integral,[21] and Z is the charge of the atomic residue of the ion. In addition, for transitions between levels of hydrogenic and helium-like ions we used an equation from Ref. 22 based on calculations in the Coulomb–Born approximation:

$$\langle \sigma v \rangle_{lu} = 10^{-8} \left(\frac{\mathrm{Ry}}{\Delta E_{lu}}\right)^{3/2} \left(\frac{E_u}{E_l}\right)^{3/2} Q_{lu} \exp(-\beta) \Psi(\beta). \tag{21}$$

where Q_{lu} is the angular factor,[22]

$$\Psi(\beta) = \sqrt{\beta} \frac{A(\beta+1)}{\beta+\chi}. \tag{22}$$

The parameters A and χ were taken from the tables in Ref. 22 or were calculated by the Atom program.[17] All the excitation rates for the ions involved in the calculations for

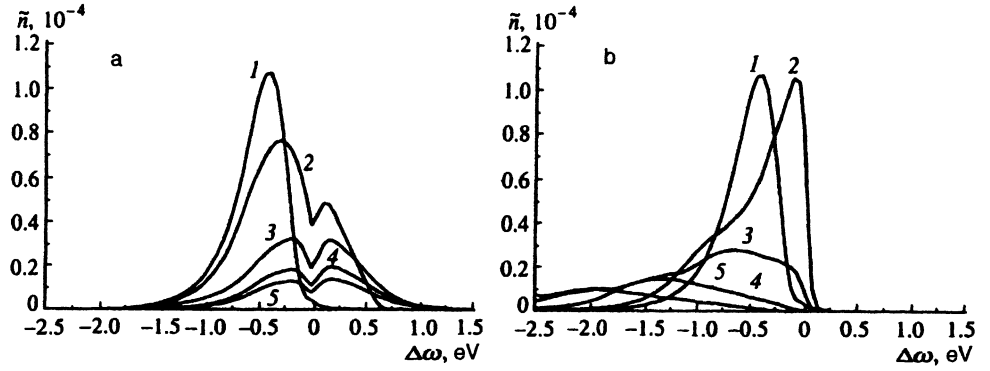

FIG. 1. Dependence of the photon occupation number in the line of the $2P_{3/2} \rightarrow 1S_{1/2}$ transition on the detuning from the undisplaced transition energy: a — in the rest (laboratory) frame; b — in a frame moving with the local plasma velocity. The curves correspond to different values of the radius: *1* — $r=0$, *2* — $r=50$ μm, *3* — $r=100$ μm, *4* — $r=150$ μm, *5* — $r=200$ μm.

an assigned range of T_e values were approximated by the formula proposed in Ref. 23 (T_e is in electron-volts):

$$\langle \sigma v \rangle_{lu} = \frac{1.58 \times 10^{-5} \exp(-\beta)}{\beta T_e^{3/2}} P(\beta), \tag{23}$$

$$P(\beta) = \exp(a_1 + a_2 \ln \beta + a_3 \ln^2 \beta + a_4 \ln^3 \beta). \tag{24}$$

The coefficients a_m in the equation for $P(\beta)$ were found by the least-squares method, and the approximation error in the required range of T_e values generally did not exceed 1–3%. The deexcitation rate was found from the detailed-balance relation.

The ionization rate of the levels of the Li-like ions was found using the Lotz formula[24]

$$\langle \sigma v \rangle_{lu} \left[\frac{\text{cm}^3}{\text{s}}\right] = 6 \times 10^{-8} \left(\frac{\text{Ry}}{E_i}\right)^{3/2} \sqrt{\beta_i} |E_1(\beta_i)|, \tag{25}$$

where $\beta_i = E_i / T_e$ and E_i is the ionization potential. For levels of the remaining ions we used the approximation[22]

$$\langle \sigma v \rangle_{lu} = 10^{-8} \left(\frac{\text{Ry}}{E_i}\right)^{3/2} Q_i \exp(-\beta_i) \Psi(\beta_i), \tag{26}$$

where Q_i is the angular factor, $\Psi(\beta) = A\sqrt{\beta}/(\beta + \chi)$, and the parameters A and χ were taken from the tables in Ref. 22. The Lotz formula was also used for levels for which there are no data in Ref. 22. In the calculations we used an approximation for the ionization rate in the form

$$\langle \sigma v \rangle_{lu} = 10^{-8} T_e^{-1/2} \exp(-\beta) P(\beta), \tag{27}$$

where $P(\beta)$ has the same functional form as in (24). The error of this approximation likewise does not exceed 1–3%. The rate of three-particle recombination was determined from the detailed-balance relation.

The photoionization cross sections were calculated from the Kramers equation with the Gaunt factors $g(\omega)$:

$$\sigma_{\text{ion}}(\omega) = 7.907 \times 10^{-18} \frac{\text{Ry}}{E_i} \frac{E_i}{\hbar\omega} \frac{m}{n} g(\omega). \tag{28}$$

where m is the number of equivalent electrons in the shell, n is the principal quantum number of the level, and $\hbar\omega$ is the photon energy. The photorecombination cross section is related to the ionization cross section by the detailed-balance relation. After averaging over the Maxwell distribution of the electrons, for the photorecombination rate we have

$$\alpha_{\text{ph}} \left[\frac{\text{cm}^3}{\text{s}}\right] = 2.599 \times 10^{-14} \frac{g_z}{g_{z+1}} \frac{m}{n} \sqrt{\frac{E_i}{\text{Ry}}} \beta^{3/2} \times \exp \beta_i \int_{\beta_i}^{\infty} \frac{e^{-x} g(x)}{x} dx. \tag{29}$$

In the present work the Gaunt factors[25] for hydrogenic ions were used for all the levels. Their tabulated values were approximated by the formula

$$g(x) = a_1 \frac{1 + a_2 \log x + a_3 \log^2 x}{1 + a_4 \log x + a_5 \log^2 x}, \tag{30}$$

where $x = \hbar\omega / E_i$.

The dielectronic recombination rate was calculated from the Burgess equation[22] and was summed for several radiative transitions that stabilize the autoionization state appearing; then it was approximated by the formula

$$\alpha_d = 10^{-13} T_e^{-3/2} \exp(-\beta) P(\beta), \tag{31}$$

where T_e is in electron-volts, $\beta = \Delta E / T_e$, and $P(\beta)$ has the same functional form as (24). The dielectronic recombination rate thus obtained was ascribed to the transition from the ground state of ion $z+1$ to the ground state of ion z. The decrease in the dielectronic recombination rate due to ionization and quenching of the autoionization states was not taken into account.

To test the calculation method for combined solution of the kinetic and radiation-transfer equations and the proposed model, we performed calculations for the conditions considered in Ref. 3. The plasma density was assumed to have the value $\rho(r) = A \exp(-r^2/L^2)$, where $A = 5 \times 10^{-4}$ g/cm^3 and $L = 9 \times 10^{-3}$ cm, and the rate was determined as $v(r) = \alpha r$, where $\alpha = 4.5 \times 10^9$ cm/s. The distribution of the electron and ion temperatures with respect to the radius had the form

$$T_{e,i} = T_{e,i}^{\max} \exp[-(r - r_{\max})^2 / L_T^2],$$

where $T_e^{\max} = 450$ eV, $T_i^{\max} = 63$ eV, $r_{\max} = 80$ μm, and $L_T = 7.2 \times 10^{-3}$ cm. Figure 1 presents the dependence of the photon occupation number in the $2P_{3/2} \rightarrow 1S_{1/2}$ line, which is the line considered in the present paper, as in Ref. 3, on the detuning from the undisplaced energy of that transition. In Fig. 1a the results are shown in the laboratory (rest) frame, and in Fig. 1b they are shown in a coordinate frame moving

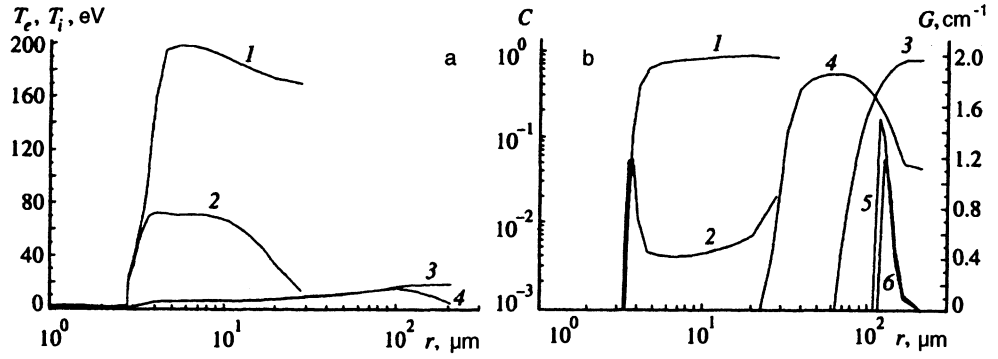

FIG. 2. Distributions of the plasma parameters in space obtained in a one-dimensional calculation. a — Temperature distributions: *1* — T_e, $t=100$ ps; *2* — T_i, $t=100$ ps; *3* — T_e, $t=500$ ps; *4* — T_i, $t=500$ ps. b — Distributions of concentrations and the gain coefficient: *1* — C[He], $t=100$ ps; *2* — C[Li], $t=100$ ps; *3* — C[He], $t=500$ ps; *4* — C[Li], $t=500$ ps; *5* — $G(4F_{5/2}\rightarrow 3D_{3/2})$, $t=500$ ps; *6* — $G(4F_{7/2}\rightarrow 3D_{5/2})$, $t=500$ ps.

with the local plasma velocity. Figure 1b is similar to Fig. 4 in Ref. 3 and exhibits good agreement for the results.

3. CALCULATION RESULTS

The calculations were performed in cylindrical geometry. The initial radius of the homogeneous target was assumed to be equal to 7.5 μm in accordance with Ref. 11. The laser pulse of Gaussian shape with respect to time and a total width of 130 ps had a peak intensity of 10^{13} W/cm^2 relative to the initial target size. The total laser energy absorbed by the plasma was 2.5 J, which corresponds to the values measured in Ref. 11. The distribution of the plasma parameters at the time of the maximum of the laser radiation pulse, as well as in later stages of expansion, is shown in Fig. 2a. The maximum value of the electron temperature is 200 eV. The temperature relaxation time is too small to completely equalize the electron and ion temperatures during the heating of the plasma by the laser radiation; however, despite the decrease in the plasma density, at the time when the maximum value of the gain coefficient is achieved (500 ps) the electron and ion temperatures become equal in practically the entire region, except for the periphery, where the plasma density decreases considerably more rapidly. Figure 2b shows the spatial distributions of the relative concentrations of He- and Li-like ions for these moments in time. It is easily seen that if the overwhelming majority of the atoms are ionized to a He-like state during the heating of the plasma (except for a narrow portion of the plasma near the thermal wave front), as a result of recombination the number of He-like ions remains appreciable as the plasma expands only at its edge, where the ionic composition is "frozen" sooner.

Figure 2b also shows the spatial distribution of the gain coefficient G (calculated with the Doppler profile) on the $4F_{5/2}\rightarrow 3D_{3/2}$ and $4F_{7/2}\rightarrow 3D_{5/2}$ transitions at the time of the gain maximum. A detailed explanation of the differences between the gain coefficients on these transitions was given in Ref. 10. A population inversion is created in a narrow peripheral region of the plasma, where the influence of the reabsorption of radiation on 3–2 transitions weakens due to the low density. In the region where inversion exists the concentration of He-like Al ions is approximately twice as great as the concentration of Li-like ions. The evolution of the spatial distribution of the gain coefficient on these transitions is shown in Figs. 3a and 3b (the numbers near the curves indicate the times in picoseconds).

The values of the populations of all the states considered, the temperatures T_e and T_i, and the density n_e found from the solution of the gas-dynamic and kinetic equations using the photon-escape-probability approximation were transferred to a program which finds the populations of levels with consideration of the radiation transfer in the lines and the continuum. Under the conditions considered here the populations of all the excited levels have steady-state values, i.e., are uniquely determined by the electron temperature T_e, the electron density n_e, and the populations of the ground states. In the case of Li-like ions, along with the $2s_{1/2}$ ground state, we also fixed the populations of the

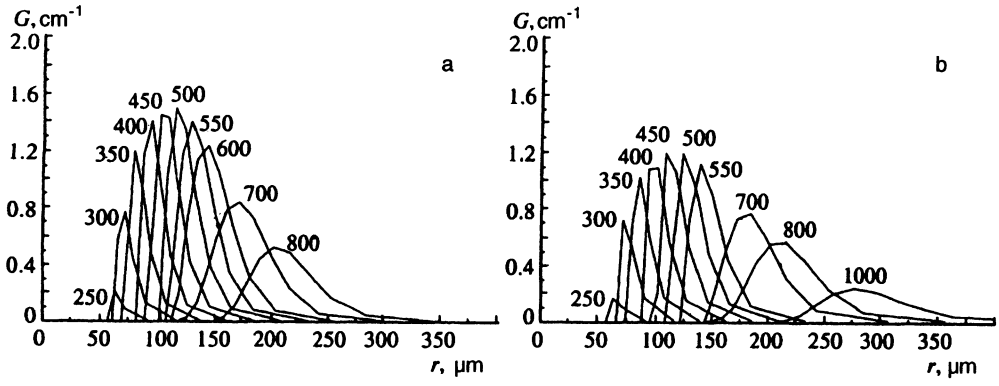

FIG. 3. Distribution of the gain coefficient with respect to the radius on the $4F\rightarrow 3D$ transitions at various moments in time (the times are indicated in picoseconds near the respective curves): a — on the $4F_{5/2}\rightarrow 3D_{3/2}$ transition; b — on the $4F_{7/2}\rightarrow 3D_{5/2}$ transition.

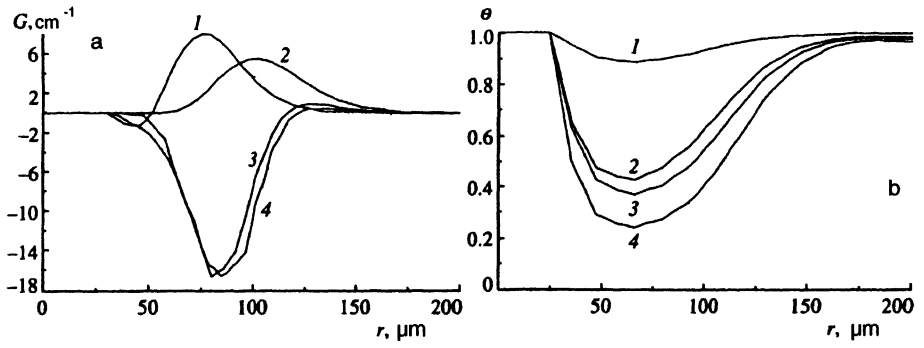

FIG. 4. Spatial distribution of the gain coefficient (a) on the $4F_{5/2}\rightarrow 3D_{3/2}$ transition: *1* — optically thin plasma ($\theta\equiv 1$), $t=400$ ps; *2* — same, $t=500$ ps; *3* — consideration of reabsorption in the photon-escape-probability approximation, $t=500$ ps; *4* — complete calculation of radiation transfer. Spatial distribution of the photon escape probability at the time $t=500$ ps (b) for several transitions: *1* — $3S_{5/2}\rightarrow 2P_{3/2}$; *2* — $3P_{3/2}\rightarrow 2S_{1/2}$; *3* — $3D_{3/2}\rightarrow 2P_{1/2}$; *4* — $3D_{5/2}\rightarrow 2P_{3/2}$.

nearby $2p_{1/2}$ and $2p_{3/2}$ levels. The system of equations (9) was modified in the following manner in accordance with the steady-state conditions:

$$\mathbf{K}'\mathbf{C}(r,t)=f, \tag{32}$$

where the matrix $\mathbf{K}'$ of the system is obtained by modifying the kinetic matrix $\mathbf{K}$, i.e.,

$$K'_{fi}=0, \quad K'_{ff}=1, \tag{33}$$

the subscript f corresponds to the states whose populations are fixed, and the remaining elements $K'_{ij}=K_{ij}$. The free term in (32)is $f_i=0$, if $i\neq f$, and $f_f=c_f$, where c_f is the value of the relative population of the state transferred from the gas-dynamic calculation. After this modification of the system of population balance equations, the conservation law of the number of particles is not, strictly speaking, obeyed. However, the calculations performed showed that the deviation of the sum $\Sigma_l C_l$ from unity is very small for the situations considered in the present work. To additionally test the correctness of the approach used, the temporal problem (9) was solved together with (8) to a time which is short enough that the populations of the fixed states cannot vary significantly, but is sufficient for the populations of the excited states to achieve steady-state values. These calculations gave identical results. One shortcoming of this approach is the need to properly select the time and the integration spacing (the time for establishing steady-state populations clearly depends on the plasma density and temperature). In addition, poorer convergence of the iterations was noted in this case during the simultaneous solution of the population balance equations and the radiation-transfer equation. We also note that the method described above for fixing the populations permits more correct transfer of the information on the populations from the essentially nonstationary gas-dynamic model to the program for solving the transfer equation than does the method used in Ref. 2, where the values of the electron and ion temperatures were varied to obtain the correct ionic composition. This unavoidably distorts the values of all the collisional constants in the population balance equations, which is totally unacceptable in the case of a recombination scheme for forming a population inversion.

Figure 4a shows the spatial distribution of the gain coefficient on the $4f_{7/2}\rightarrow 3D_{5/2}$ transition obtained from the gas-dynamic model using escape probabilities (curve *1*), as well as by solving the radiation-transfer equation together with the population kinetics (curve *2*). Curves *1* and *2* correspond to a time of 500 ps. For comparison, Fig. 4a also shows the spatial distribution of the gain coefficient on the same transition obtained on the basis of the gas-dynamic model under the assumption of an optically transparent plasma ($\theta=1$) for times equal to 400 ps (curve *3*) and 500 ps (curve *4*). It is easy to see the striking difference between the distributions and the values of the gain coefficient when the reabsorption of radiation in the spectral lines is taken into account and when it is not. The spatial distribution of the photon escape probabilities for a series of $3\rightarrow 2$ transitions is shown in Fig. 4b. The gain coefficient reaches a maximum at the value of the photon escape probability for the radiative transitions which sweep out the lower working level, $\theta=0.7$–0.9, i.e., only in the practically transparent region. In the more peripheral regions of the plasma the increase in the escape probability does not compensate the decrease in the populations of the working levels caused by the general decline in the plasma density. It is seen from Fig. 4a that in the region of the plasma where the reabsorption of radiation on the $3\rightarrow 2$ transitions is great ($\theta\ll 1$), the values of the gain coefficient (which are negative and correspond to absorption) on the $4f_{7/2}\rightarrow 3D_{5/2}$ transition calculated from the gas-dynamic model using escape probabilities and from the complete model practically coincide. This is a good argument supporting the conclusion that both models faithfully describe the reabsorption of radiation in resonance lines within a plasma with strong absorption.

At the same time, in the region of practical interest, where $G>0$ (amplification), the maximum values of the gain coefficient obtained by these two methods differ by a factor of almost 2 (Fig. 5). We assume that this difference is due to the extremely high sensitivity of the value of G to the magnitude of the inversion $1-g_u C_l/g_l C_u$, which, in turn, is determined by the radiation transfer in the lines of the transitions which sweep out the lower working level ($3D_{5/2}$ in the present case). A population inversion appears in the region of the extremely abrupt decline in the populations of the excited states mainly due to the decrease in the recombination pumping, which is proportional to $N_e^2 N_i$. As a result, even small differences in the numerical methods can produce considerable differences in G. We note that the value obtained in the experiments in Ref. 11 is significantly greater than both values shown in Fig. 5. This is typical of all the theories which take into account reabsorption in the photon-escape-probability approximation. We also note that the

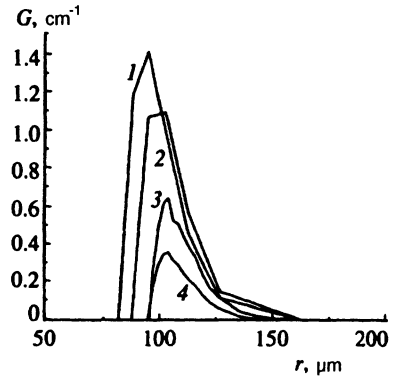

FIG. 5. Comparison of the gain coefficient G on the $4F \rightarrow 3D$ transitions calculated in the photon escape probability approximation in a line and for the complete model of radiation transfer at 400 ps: *1* — for the $4F_{5/2} \rightarrow 3D_{3/2}$ transition in the θ approximation; *2* — same for the $4F_{7/2} \rightarrow 3D_{5/2}$ transition; *3* — on the $4F_{5/2} \rightarrow 3D_{3/2}$ transition for the complete model; *4* — same for the $4F_{7/2} \rightarrow 3D_{5/2}$ transition.

photon-escape-probability (θ) approximation does not contain a small parameter, which would make it possible to evaluate its region of applicability. The accuracy of this approximation was investigated for the case of a stationary medium with a large optical thickness in Ref. 26, where it was shown that the accuracy of the determination of the population of the upper level is about 20% in the case of a uniform distribution of the plasma parameters and that the difference between the exact solution and the solution obtained in the escape-probability approximation can reach 100% in the case of a nonuniform distribution. Obviously, in the case of a laser plasma we are dealing with an extremely nonuniform distribution of the parameters. Another important point is that a population inversion appears at times when the photon escape probability becomes of the order of unity. Apparently, under these conditions the escape-probability approximation does not provide sufficient accuracy in finding populations.

The results of the calculations of G on the $4F \rightarrow 3D$ transition are similar to those presented for the $4F \rightarrow 3D$ transition. The difference is confined to the smaller value of the gain coefficient on this transition.

4. CONCLUSIONS

The results obtained in the present work allow us to draw the following conclusions. The accuracy of a self-consistent description within the standard approach involving the solution of the gas-dynamic equations together with the population kinetics, in which the role of the reabsorption of the resonant radiation is taken into account in the photon-escape-probability (θ) approximation in an inhomogeneous moving medium, was tested for a recombination-pumped x-ray laser in the case of a Li-like Al ion. It was shown that for locally optically thick lines [where $\theta(r) \ll 1$] the photon-escape-probability approximation is in satisfactory agreement with the results of the numerical solution of a combined system of equations describing the kinetics and resonant radiation transfer in an inhomogeneous moving plasma. This result is consistent with the data in Refs. 27 and 28. The main difference in the present work is confined to the more systematic calculation of the population kinetics during the combined solution of the line radiation-transfer equation. For example, in Ref. 29 the populations of the excited states used to solve the radiation-transfer equation were taken from calculations of the kinetics in the photon-escape-probability approximation, and in Ref. 3 the ionic composition was fixed by adjusting the temperatures of the charged particles, which can alter the entire population kinetics of the excited states. The procedure proposed in this paper maintains the temperature values obtained by solving the gas-dynamic equations and does not dictate the values of the populations of the excited levels. As a result, it was found that the accuracy of the photon-escape-probability approximation is not satisfactory for describing the gain coefficient on the $5F \rightarrow 3D$ and $4F \rightarrow 3D$ transitions in a Li-like Al ion appearing on the periphery of an expanding plasma, where the value of θ is close to unity, and the system of kinetic and radiation-transfer equations must be systematically solved on top of the inhomogeneous background of the distribution of the gas-dynamic parameters of the plasma to obtain the correct value of the gain coefficient. The more rigorous approach diminishes the gain coefficient by more than two fold, leading to poor agreement between the calculation and experiment. Therefore, to elucidate the mechanism for creating inversion in a scheme of recombination x-ray lasers there is need both for additional experiments, in which, apart from the gain coefficient, the spatial distribution of the ionic composition of the plasma must be measured with temporal resolution, and for consideration of all the processes occurring in the presence of sharp gradients in the distribution of the ionic composition, such as the diffusion of, for example, He-like ions into a region where amplification is observed, which can increase the calculated value of G. The latter is especially important for explaining the gain on the $5F \rightarrow 3D$ transition, where the observed value $G_{5-3} \sim 1$ cm^{-1} is significantly greater than the calculated value even in the absence of radiation reabsorption.

This work was performed with partial support from the Soros International Science Foundation (the Grant was furnished by the American Physical Society) and as part of Project 076-95 of the International Scientific-Technical Center.

[1] D. L. Matthews, P. L. Hagelstein, M. D. Rosen, *et al.*, Phys. Rev. Lett. **54**, 110 (1985).
[2] D. C. Eder, Phys. Fluids B **1**, 2462 (1989).
[3] D. C. Eder and H. A. Scott, J. Quant. Spectrosc. Radiat. Transfer **45**, 189 (1991).
[4] A. V. Borovskiy, P. B. Holden, M. T. M. Lightbody, and G. J. Pert, J. Phys. B **25**, 4991 (1992).
[5] V. Sobolev, Sov. Astron. **1**, 678 (1957).
[6] G. B. Rybicki and D. G. Hummer, Astrophys. J. **254**, 767 (1982).
[7] F. E. Irons, J. Quant. Spectrosc. Radiat. Transfer **43**, 107 (1990).
[8] A. I. Shestakov and D. C. Eder, J. Quant. Spectrosc. Radiat. Transfer **42**, 483 (1989).
[9] G. B. Rybicki and D. G. Hummer, Astrophys. J. **274**, 380 (1983).
[10] V. Makhrov, V. Roerich, A. Starostin *et al.*, J. Phys. B **27**, 1899 (1994).
[11] A. Carillon, M. J. Edwards, M. Grande *et al.*, J. Phys. B **23**, 147 (1990).
[12] *Reviews of Plasma Physics, Vol. 1*, edited by M. A. Leontovich (Consultants Bureau, New York, 1963) [Russ. original, Atomizdat, Moscow, 1963, p. 183].

[13] D. Mihalas, *Stellar Atmospheres*, 2nd edn. (W. H. Freeman, San Francisco, 1978) [Russ. transl., Mir, Moscow, 1982].
[14] B. N. Chetverushkin, *Mathematical Modeling of Problems in Radiating Gas Dynamics* [in Russian] (Nauka, Moscow, 1985).
[15] R. D. Cowan, *The Theory of Atomic Structure and Spectra* (Univ. of California Press, Los Angeles, 1981).
[16] H. Guennou and A. Sureau, J. Phys. B **20**, 919 (1987).
[17] L. A. Vaĭnshteĭn and V. P. Shevel'ko, *Structure and Characteristics of Ions in a Hot Plasma* [in Russian] (Nauka, Moscow, 1986).
[18] C. E. Moore, *Atomic Energy Levels, Vols. 1-3* (Natl. Bur. Stand., Washington, D. C., 1949, 1950, 1952).
[19] H. Van Regemorter, Astrophys. J. **136**, 906 (1962).
[20] V. A. Bazylev and M. I. Chibisov, in *Reviews of Plasma Physics, Vol. 12*, edited by B. B. Kadomtsev (Consultants Bureau, New York, 1987) [Russ. original, Atomizdat, Moscow, 1982, p. 30].
[21] M. Abramowitz and I. A. Stegun (editors), *The Handbook of Mathematical Functions* (Dover, New York, 1976) [Russ. transl., Mir, Moscow, 1969].
[22] I. I. Sobelman, L. A. Vainshtein, and E. A. Yukov, *Excitation of Atoms and Broadening of Spectral Lines* (Springer-Verlag, Berlin, 1981).
[23] P. L. Hagelstein, Ph. D. Thesis, Lawrence Livermore National Laboratory, University of California, Livermore, California, CRL-53100 (1981).
[24] W. Lotz, Z. Phys. **232**, 101 (1970).
[25] W. J. Karzas and R. Latter, Astrophys. J. Suppl. **6**, 167 (1961).
[26] A. P. Napartovich, Teplofiz. Vys. Temp. **9**, 26 (1971) [High Temp. (USSR) **9**, 23 (1971)].
[27] Y. T. Lee, R. A. London, and G. B. Zimmerman, Phys. Rev. B **2**, 2731 (1990).
[28] D. C. Eder, H. A. Scott, S. Maxon, and R. A. London, Appl. Opt. **31**, 4962 (1992).
[29] A. Djaoui, S. J. Rose, and J. S. Wark, Annual Reports, Rutherford Appleton Laboratory (1994), pp. 64, 65.

Translated by P. Shelnitz